

On morphological color texture characterization

ERCHAN APTOULA and SÉBASTIEN LEFÈVRE

UMR-7005-CNRS-LSIT, Université Louis Pasteur, Illkirch, France
{[aptoula](mailto:aptoula@lsit.u-strasbg.fr),[lefevre](mailto:lefevre@lsit.u-strasbg.fr)}@lsit.u-strasbg.fr

Abstract We investigate the combined use of multiple structuring elements with the standard morphological texture characterization tools, namely morphological covariance and granulometry. The resulting operator is applied to both grayscale and color images in the context of texture classification. As to its extension to color texture data, it is realized by means of a weighting based reduced vector ordering in the I HLS color space, equipped with genetically optimized arguments. The classification experiments based on this framework are carried out with the publically available Outex13 texture database, where the proposed feature extraction scheme outperforms the univariable versions of the operators under consideration.

Keywords: multivariate mathematical morphology, texture, granulometry, covariance, color ordering.

1. Introduction

Mathematical morphology (MM) offers a variety of tools for texture characterization, such as *granulometry*, *morphological covariance*, *orientation maps*, etc. The first two in particular have been employed successfully in a number of texture analysis applications [3, 7, 22, 23].

More precisely, granulometry is a powerful tool based on the “sieving” principle, implemented by means of successive openings and/or closings with structuring elements (SE) of various sizes, hence it is capable of extracting shape and size characteristics from textures. Morphological covariance on the other hand, is based on erosions with pairs of points separated by vectors of various lengths, and provides information on the coarseness, anisotropy as well as periodicity of its input.

In this paper, we concentrate on these two operators, and specifically on the combined exploitation of their SE variables: size, distance and direction. Since the original size-only definition of pattern spectra [13], these operators have been extended in various ways (e.g., color, multivariate, attribute based versions, etc.). Relatively recent applications have explored for instance the combination of SE shape and size as far as granulometry is concerned [24, 25], hence leading to a feature matrix rather than a vector, that describes the combined size and shape distribution of its input. As to covariance, the

coupled use of SE pair distance and direction makes it possible to exploit the anisotropic properties of textures additionally to their periodicity [12, 23].

Here we investigate the ways of combining the complementary information extracted by these two operators (e.g., concatenation, dimension reduction, etc.), and propose a hybrid of the two, where SE couples are varied in terms of size, direction as well as distance. The proposed combination scheme is compared in terms of classification accuracy, against the standard definitions, using the publically available Outex13 color texture database. The so far obtained experimental results show that it leads to an improvement over the usual concatenation of feature vectors.

Furthermore, as far as the extension of this operator to color images is concerned, since MM is based on complete lattice theory, a vector ordering mechanism becomes necessary. Hence, we propose a weight based reduced vector ordering, defined on the improved HLS (IHLS) color space, designed specifically for the purpose of color texture classification. This approach makes it possible to optimize, for instance through genetic algorithms, the weight of each component adaptively, according to the training set under consideration.

The rest of the paper is organized as follows. Section 2 introduces briefly granulometry and covariance, and then elaborates on the combination of their variables. In Section 3, the problem of extending morphological operators to multivariate images is discussed, and the proposed ordering is detailed. Next, Section 4 presents the experimental results that have been obtained with the Outex13 database. Finally, Section 5 is devoted to concluding remarks.

2. Morphological texture characterization

In this section, we start by recalling the basic texture categories along with their perceptual characteristics, and then the covariance and granulometry operators are introduced. Moreover, the combination of multiple SE related variables is discussed.

2.1 Texture properties

According to the pioneering taxonomy work of Rao [19], textures can be classified with respect to their spatial distribution of details into the following four categories (Figure 1).

Strongly ordered: Textures consisting of the repetitive placement of their primitive elements according to a particular set of rules.

Weakly ordered: Textures possessing a dominant local orientation, which can however vary at a global level.

Disordered: Textures lacking any repetitiveness and orientation, and usually described on the basis of their roughness.

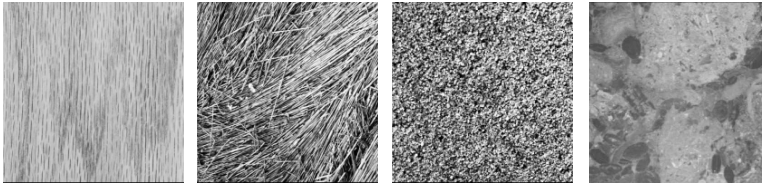


Figure 1. Texture examples from the Brodatz album [5], from left to right, strongly ordered, weakly ordered, disordered and compositional.

Compositional: Textures that do not belong to any of the previous categories, and exhibit a combination of their characteristics.

In an effort to determine efficient features, capable of discriminating among the members of these categories, Rao and Lohse [20] have conducted psycho-physical experiments, and identified *regularity* (or *periodicity*), *directionality* and *complexity* as the most important perceptual texture characteristics, as far as human observers are concerned. With the subsequent work of Chetverikov [6] and Mojsilovic et al. [16], *overall color* and *color purity* were added to this list.

2.2 Morphological covariance

This operator was initially proposed [14, 15, 22] as the equivalent in MM of the autocorrelation operator. The morphological covariance K of an image f , is defined as the volume Vol , i.e., sum of pixel values, of the image, eroded by a pair of points $P_{2,v}$ separated by a vector \vec{v} :

$$K(f; P_{2,v}) = \text{Vol}(\varepsilon_{P_{2,v}}(f)), \quad (1)$$

where ε represents the erosion operator. In practice, K is computed for varying lengths of \vec{v} , and most often the normalized version is used for measurements:

$$K^n(f) = \text{Vol}(\varepsilon_{P_{2,v}}(f)) / \text{Vol}(f). \quad (2)$$

In the light of the aforementioned perceptual properties of textures, given the resulting uni-dimensional covariance series, one can gain insight into the structure of a given image [23]. In particular, the periodic nature of covariance is strongly related to that of its input. Furthermore, the period of periodic textures can easily be determined by the distance between the repeated peaks, that appear at multiples of the sought period; whereas the size of the periodic pattern can be quantified by means of the width of the peaks. In other words, their sharpness is directly proportional to the thinness of the texture patterns appearing in the input. Likewise, the initial slope at the origin provides an indication of the coarseness, with quick drop-off corresponding to coarse textures.

In order to obtain additional information on the directionality of f , one can plot against not only different lengths of \vec{v} , but orientations as well [12].

2.3 Granulometry

Granulometry [14, 15] as a term belongs to the field of materials science, where the granularity of materials is determined by passing them through sieves. Using the same principle, this operator consists in studying the amount of image detail removed by applying morphological openings γ_λ and/or closings ϕ_λ of increasing size λ . The volumes of the opened (or closed) images are then plotted against λ , or more usually their discrete derivative $\text{Vol}(\gamma_\lambda - \gamma_{\lambda+1})$, i.e., *pattern spectrum*. The normalized version of the operator can be written as:

$$G^n(f) = \text{Vol}(\gamma_\lambda(f)) / \text{Vol}(f). \quad (3)$$

For unbiased measurements, the volume computation may be reduced only to the area affected by the operator. As a featuring tool, granulometry provides information on the shape and size of ordered textures, and regularity of disordered textures [4, 23]. Furthermore, both operators can be applied on a local or global level.

2.4 Proposed approach

Indeed, considering the fundamental perceptual texture properties mentioned in Section 2.1, morphological covariance and granulometry provide invaluable, yet complementary information on their input. More precisely, covariance extracts a feature vector containing information on periodicity and directionality, whereas granulometry concentrates rather on the granularity of its input. Consequently both are necessary in the general case for an efficient texture description.

However, their combination is rather ambiguous, as it can be realized in a variety of ways. The obvious method, is to calculate independently each feature vector and then employ their concatenation. We propose here an alternative way, which consists in unifying the two operators' functionalities by varying in parallel multiple SE properties. As previously mentioned, the use of multivariate granulometry and covariance has already been reported, specifically, in the form of combined SE direction and distance [9], as far as covariance is concerned, and shape and size combination with granulometry [24, 25].

We choose to implement with this purpose a combination of SE size, direction and distance (Figure 2). For practical purposes, we replace the erosion (ε) operator of covariance (2) with an opening (γ). Of course, on the contrary of granulometry it is also necessary to employ SE pairs, so that periodicity information may be extracted. Hence the following hybrid expression is obtained:

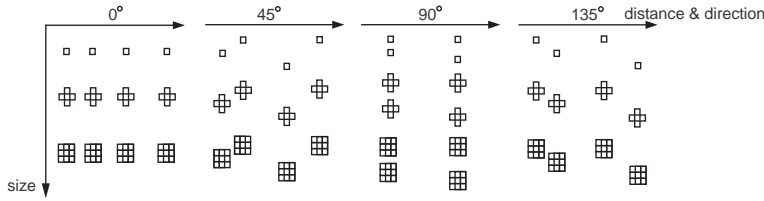


Figure 2. Illustration of structuring element pair variations, with respect to size, direction and distance.

$$GK^n(f) = \text{Vol}(\gamma_{P_{\lambda,v}}(f)) / \text{Vol}(f), \quad (4)$$

where $P_{\lambda,v}$ denotes a pair of SEs of size λ separated by a vector \vec{v} . However, it should be noted that as the sieving principle of multiple morphological openings is satisfied if, and only if the SE is a compact convex set [15], this combination no longer qualifies as a granulometry. In practice, only the four basic directions ($0^\circ, 45^\circ, 90^\circ, 135^\circ$) are of importance, thus it was chosen to integrate directional variation with distance as shown in Figure 2. Of course, in case directionality becomes particularly significant one can always separate it as an additional dimension representing a finer distinction of directions, or even add one more dimension for shape distributions, where different SE shapes (e.g., disc approximation, square, lines, etc.) are also employed along with direction, size and distance.

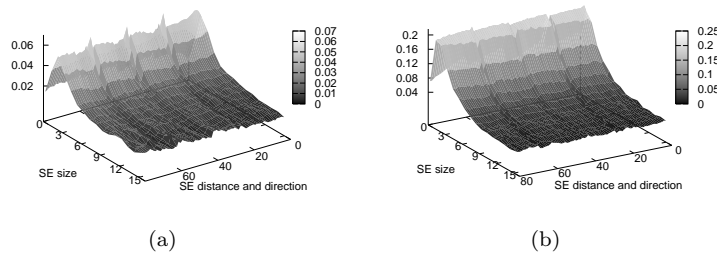


Figure 3. Plot of the feature matrices resulting from the application of expression (4) on the strongly ordered (left) and disordered (right) texture of Figure 1.

Figure 3 presents the plots of the resulting features matrices, as applied to the strongly ordered and disordered textures of Figure 1. Although their size distributions are rather similar, their directionality and periodicity are clearly distinct.

Moreover, as far as classification is concerned, feature vector or matrix size is of primary importance, since redundant information may eventually

be present and disrupt the overall process. Even with the moderate sizes used in practice, the resulting feature set can easily become excessively large. That is why dimension reduction techniques, such as principal component analysis (PCA), as it will be shown in Section 4, could become necessary. Before testing the proposed approach, as well as the different ways of its use, in the next section a way of extending morphological operators, along with the proposed hybrid operator, to color images is presented.

3. Extending to color images

As previously mentioned, color is an integral part of texture description, and several ways of extracting color features have been reported, e.g., color histograms, color correlograms, etc. According to Palm [18], these techniques can be classified into the following three categories.

Parallel approach: Color and intensity information is processed separately. For instance a color histogram along with a co-occurrence matrix.

Sequential: Color information is first transformed into a greyscale form, which is then processed with the tools available for intensity images.

Integrative: The color channels are processed either separately or simultaneously.

Here we choose to implement the third approach. The extension of morphological operators to color and more generally to multivariate images is still an open problem. Specifically, since the morphological framework is based on complete lattice theory [21], it is theoretically possible to define morphological operators on any type of image data, as long as a complete lattice structure can be introduced on the image intensity range. In other words, at least a partial vector ordering is required. Several approaches have been proposed with this purpose (e.g., marginal ordering, r-orderings, c-orderings, etc.), a comprehensive survey of which can be found in [1].

3.1 Color space

The choice of color space is of fundamental importance, as it can largely influence the end results [11]. Here, we choose to follow the trend of the last years in the domain of color morphology, and employ a polar color space based on the notions of hue ($h \in [0, 2\pi]$), saturation ($s \in [0, 1]$) and luminance ($l \in [0, 1]$). More precisely, although most polar color spaces are essentially just a more intuitive description of the RGB color cube, several implementations exist, e.g., HSV, HSB, HLS, HSI, etc. [8]. According to Hanbury and Serra [10], the cylindrical versions of these spaces have serious inconsistencies and are inappropriate for quantitative color image processing. Hence we make our color space choice in favor of the *improved HLS* space (IHLS) [10] using the L1 norm, which employs the original bi-conic version of HLS.

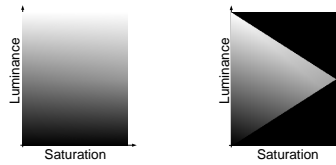


Figure 4. Vertical semi-slice of the cylindrical HLS (left) and bi-conic IHLS (right) color spaces.

As illustrated in Figure 4, one of the most important drawbacks of the cylindrical HLS space is the unintuitive definition of saturation. Specifically, it is possible to have maximized saturation values for zero luminance. This inconvenience, as well as the dependence of saturation on luminance are remedied with the IHLS space, where the maximal allowed value for saturation is limited in relation to luminance. Therefore, in order to benefit from the advantages of polar spaces in the context of multivariate morphology, the ordering of IHLS color vectors is necessary.

3.2 Ordering color vectors

For the sake of simplicity, we have omitted the hue component at this stage of our research from the ordering process, and instead we concentrate on the relations of luminance (l) and saturation (s) (color purity). Luminance is well known to account for the intensity variations and consequently, it is often sufficient for the recognition of most objects, whereas color has a rather auxiliary contribution. These two components may be ordered in a variety of ways, for instance marginally, lexicographically, etc. A marginal ordering strategy in this case:

$$\forall \mathbf{c}, \mathbf{c}' \in [0, 1]^2, \quad \mathbf{c} \leq \mathbf{c}' \Leftrightarrow c_1 \leq c'_1 \wedge c_2 \leq c'_2, \quad (5)$$

is rather inappropriate as it does not take into account inter-channel relations. A lexicographical approach on the other hand, with luminance at top position:

$$\forall \mathbf{c}, \mathbf{c}' \in [0, 1]^2, \quad \mathbf{c} \leq \mathbf{c}' \Leftrightarrow c_1 \leq c'_1 \vee (c_1 = c'_1 \wedge c_2 \leq c'_2), \quad (6)$$

prioritizes excessively the first component, since the second dimension (i.e., saturation) does not contribute to the outcome of vector comparisons unless an equality takes place at the first.

We choose to use a reduced or R-ordering where color vectors are first reduced into scalar values and then ranked according to their natural scalar order:

$$\forall \mathbf{c}, \mathbf{c}' \in [0, 1]^2, \quad \mathbf{c} \leq \mathbf{c}' \Leftrightarrow g(\mathbf{c}) \leq g(\mathbf{c}'). \quad (7)$$

Obviously the main issue at this point is the choice of the scalarization function $g : [0, 1]^2 \rightarrow \mathbb{R}$. In order to efficiently combine the information

contained in saturation and luminance channels, their relations need to be taken into account. Specifically, given the bi-conic form of IHLS, saturation can reach its maximal value for medium luminance levels, whereas it is of minimal importance for extreme levels (i.e., either too dark or too bright). In order to model this relation we choose to use the sigmoid based transition proposed in [2]:

$$l \in [0, 1], \quad h(l) = \begin{cases} \frac{1}{1+\exp(-k_L(l-l_l))} & \text{if } l \leq 0.5, \\ \frac{1}{1+\exp(k_L(l-l_u))} & \text{if } l \geq 0.5, \end{cases} \quad (8)$$

where the slope $k_L = 10$, and the lower and upper offsets are respectively $l_l = 0.25$ and $l_u = 0.75$. Its plot is given in Figure 5. The arguments of $h(l)$ were set empirically, and divide the luminance range roughly in three regions, with the middle corresponding to important saturation levels.

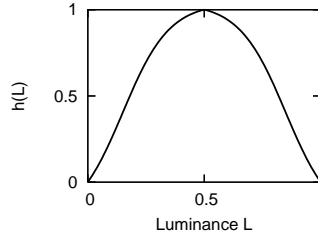


Figure 5. Plot of the weighting function $h(l)$ for the importance of color purity in relation to luminance.

Furthermore, the main problem consists in determining the influence of each component. In other words, in what amount are we to use luminance and saturation when comparing vectors? In the ideal case, one would follow an image or vector specific approach, for example by increasing the contribution of saturation if the image or vectors under consideration are highly saturated. However, this method is in our opinion suitable for intra-image problems such as filtering, but ill suited for inter-image problems, such as texture classification. It results in using different weights for each component depending on the vectors or processed image, hence leading to a highly adaptive approach, which undermines the comparability of the calculated feature sets.

Therefore, we propose to follow a strategy where the contribution of each component is dependent on the image database under consideration. More precisely, g is defined as:

$$w_l, w_s \in \mathbb{R}, \quad \forall (l, s) \in [0, 1]^2, \quad g(l, s) = w_l \times l + w_s \times h(l) \times s, \quad (9)$$

where $w_l + w_s = 1$ are the weights of luminance and saturation respectively. These weights are to be determined by means of a genetic algorithm, or any other means of unsupervised optimization. Specifically, given the training

set of textures, the values of w_l and w_s are to be set to their values minimizing the cost function w of features, that in turn minimizes the distance of features among textures of the same class, and maximizes the distance of textures belonging to distinct classes:

$$w = dist_{intra-class} + (1 - dist_{inter-class}). \quad (10)$$

Consequently, the color ordering becomes specific to the image database under consideration. Of course this principle is by no means limited to textures and can be applied in a likewise fashion for optimizing for instance the ordering of multispectral vectors in remote sensing images. Application results are given in the next section.

4. Results

In this section, we present the results that have been obtained using the color textures of Outex13 (Figure 6) [17]. This set consists of 68 textures, where every image has been divided into 20 non-overlapping sub-images, each of size 128×128 pixels, thus producing a total of 1360 images, which are evenly divided as training and test sets. We compare four different feature extraction schemes with both grayscale and color images. Specifically, we test features computed using a granulometry (Granulometry) (3), morphological covariance (Covariance) (2), their concatenation (Concatenated) and finally their proposed combined form (Combined).

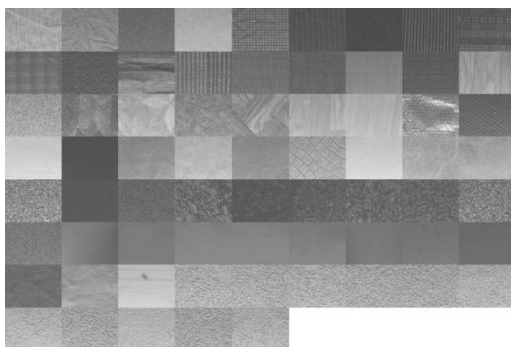


Figure 6. Examples of the 68 textures of Outex13 [11].

More precisely, for granulometry square shaped SEs have been employed, where a SE of size k has a side of $2k + 1$ pixels, and k varied from 1 to 30 in steps of size 2. As to covariance, the four basic directions have been used ($0^\circ, 45^\circ, 90^\circ, 135^\circ$) in combination with distances varying from 1 to 20. For their concatenated as well as proposed combined form (4) the same arguments were in place. The 80×25 feature matrix that has resulted from

the combination option, was reduced into a matrix of size 2x80 by means of a PCA transform and preserving only the first two dimensions. For grayscale computations the luminance component of IHLS has been used, while for the processing of color information the vectorial versions of operators were implemented, based on the ordering (7), the weights of which have been set in two ways. Besides using fixed values (*Color*: $w_l = w_s = 0.5$), the optimization described in Section 3.2 has been also implemented (*Color-optimized*). The image set has been classified using a kNN classifier with $k = 1$ and the Euclidean distance as a similarity metric.

The classification accuracies, computed as the fraction formed by the number of successful classifications divided by the total number of subjects, are given in table Table 1. Globally, one can immediately remark the positive, though comparably to intensity, small effect of using color information. A result which asserts the auxiliary role of color in texture recognition. Moreover, covariance systematically outperforms granulometry, hence showing the higher pertinence of periodicity and directionality with this database, compared to granularity. The combination of the two operators by means of a concatenation improves the accuracy levels, while the proposed hybrid operator provides the overall best results, both with color as well as grayscale images. Additionally, according to the obtained values, the optimization scheme appears to result in database specific feature vectors, hence improving the overall performance.

Table 1. Classification accuracies (%) for the Outex 13 textures.

<i>Features</i>	<i>Grayscale</i>	<i>Color</i>	<i>Color optimized</i>
Granulometry	67.53	68.78	72.03
Covariance	73.82	76.92	80.46
Concatenated	77.75	79.93	83.74
Combined	83.53	85.53	88.13

5. Conclusion

As a fundamental problem of computer vision, several approaches have been developed for texture description. Their extension to color images however is still an open issue. In this paper, we have proposed a method for combining the complementary information provided by the two basic texture featuring tools offered by mathematical morphology. This combination by means of varying multiple SE variables has the advantage of better capturing, with respect to a mere concatenation, the three essential texture properties: periodicity, directionality and complexity. Its extension to color data has been realized using a reduced ordering in the IHLS space. The use of weights results in a flexible solution that makes it possible for each image channel to

contribute to the vector comparison outcome. Furthermore, optimization methods may be employed for rendering this ordering data specific.

The experiments that have been carried out on the Outex13 database, have provided indications on the proposed methods' practical interest. Future work will concentrate on the additional exploitation of shape information. Moreover, the use of the hue component holds further potential of improving the efficiency for the computed feature vectors.

References

- [1] E. Aptoula and S. Lefèvre, *A comparative study on multivariate mathematical morphology*, Pattern Recognition **40** (November 2007), no. 11, 2914–2929, DOI 10.1016/j.patcog.2007.02.004.
- [2] ———, *On the morphological processing of hue*, submitted to Image and Vision Computing (2007).
- [3] A. Aubert, D. Jeulin, and R. Hashimoto, *Surface texture classification from morphological transformations*, International Symposium on Mathematical Morphology (Palo Alto, USA, June 16–18, 2000) (J. Goutsias, L. Vincent, and D. S. Bloomberg, eds.), Kluwer Academic Publishers, 2000, Mathematical morphology and its applications to Image and Signal Processing, pp. 253–252.
- [4] S. Batman and E. R. Dougherty, *Size Distributions for Multivariate Morphological Granulometries: Texture Classification and Statistical Properties*, Optical Engineering **36** (May 1997), no. 5, 1518–1529.
- [5] P. Brodatz, *Textures: a photographic album for artists and designers*, Dover, New York, 1966.
- [6] D. Chetverikov, *Fundamental structural features in the visual world*, International Workshop on Fundamental Structural Properties in Image and Pattern Analysis, (Budapest, Hungary, September 6–7, 1999), pp. 47–58.
- [7] G. Fricout and D. Jeulin, *Texture classification from their morphological properties*, International Conference on Metrology and Properties of Engineering (Halmstad University, Sweden, September 2003), pp. 42–55.
- [8] R. C. Gonzalez and R. E. Woods, *Digital Image Processing*, Addison-Wesley, New York, 1992.
- [9] A. Hanbury, U. Kandaswamy, and D. A. Adjeroh, *Illumination-invariant Morphological Texture Classification*, International Symposium on Mathematical Morphology (Paris, France, April 18–20, 2005) (C. Ronse, L. Najman, and E. Decenci re, eds.), Springer-Verlag, Dordrecht, Netherlands, 2005, Mathematical Morphology: 40 years on, pp. 377–386.
- [10] A. Hanbury and J. Serra, *Colour Image Analysis in 3D-polar Coordinates*, International Conference on Image Processing and its Applications (Magdeburg, Germany, September 2003), pp. 124–131.
- [11] T. M enp    and M. Pietik  inen, *Classification with color and texture: jointly or separately?*, Pattern Recognition **37** (August 2000), no. 8, 1629–1640.
- [12] A. Mauricio and C. Figuerido, *Texture analysis of grey-tone images by mathematical morphology: a nondestructive tool for the quantitative assessment of stone decay*, Mathematical Geology **32** (2000), no. 5, 619–642.
- [13] P. Maragos, *Pattern spectrum and multiscale shape representation*, IEEE Transactions on Pattern Analysis and Machine Intelligence (1989), no. 11, 701–715.
- [14] G. Matheron, *El ments pour une Th orie des Milieux Poreux*, Masson, Paris, 1967.

- [15] ———, *Random Sets and Integral Geometry*, J. Wiley, New York, 1975.
- [16] A. Mojsilović, J. Kovačević, D. Kall, R. J. Safranek, and S. K. Ganapathy, *The vocabulary and grammar of color patterns*, IEEE Transactions on Image Processing **9** (2000), no. 3, 417–431.
- [17] T. Ojala, T. Mäenpää, M. Pietikäinen, J. Viertola, J. Kyllönen, and S. Huovinen, *Outex: New framework for empirical evaluation of texture analysis algorithms*, International Conference on Pattern Recognition (Quebec City, Canada, August 2002), pp. 701–706.
- [18] C. Palm, *Color texture classification by integrative co-occurrence matrices*, Pattern Recognition **37** (May 2004), no. 5, 965–976.
- [19] A. R. Rao, *A Taxonomy for Texture Description and Identification*, Springer-Verlag, New York, 1990.
- [20] A. R. Rao and G. L. Lohse, *Identifying high level features of texture perception*, CVGIP: Graphical Models and Image Processing **55** (1989), no. 3, 218–233.
- [21] C. Ronse, *Why mathematical morphology needs complete lattices*, Signal Processing **21** (October 1990), no. 2, 129–154.
- [22] J. Serra, *Image Analysis and Mathematical Morphology Vol I*, Academic Press, London, 1982.
- [23] P. Soille, *Morphological Image Analysis : Principles and Applications*, Springer-Verlag, Berlin, 2003.
- [24] E. R. Urbach, N. J. Boersma, and M. H. F. Wilkinson, *Vector-attribute filters*, International Symposium on Mathematical Morphology, (Paris, France, April 18–20, 2005) (C. Ronse, L. Najman, and E. Decencière, eds.), Springer-Verlag, Dordrecht, Netherlands, 2005, Mathematical Morphology: 40 years on, pp. 95–104.
- [25] E. R. Urbach, J. B. T. M. Roerdink, and M. H. F. Wilkinson, *Connected Shape-Size Pattern Spectra for Rotation and Scale-Invariant Classification of Gray-Scale Images*, IEEE Transactions on Pattern Analysis and Machine Intelligence **29** (February 2007), no. 2, 272–285.